Journal of Power Sources 270 (2014) 59–67

Contents lists available at ScienceDirect

Journal of Power Sources

journal homepage: www.elsevier.com/locate/jpowsour

The through-plane thermal conductivity and the contact resistance of the components of the membrane electrode assembly and gas diffusion layer in proton exchange membrane fuel cells

N. Alhazmi*, D.B. Ingham, M.S. Ismail, K. Hughes, L. Ma, M. Pourkashanian

Centre for Computational Fluid Dynamics, Energy Technology Innovation Initiative, The University of Leeds, LS2 9JT, UK

HIGHLIGHTS

- The thermal conductivity of the membrane was comparable in both directions.
- The through-plane thermal conductivity of the membrane decreases with temperature.
- The through-plane thermal conductivity of the GDL decreases with temperature.
- The through-plane thermal conductivity of the GDL increases with compression.
- The thermal conductivity of the catalyst was comparable in both directions.

ARTICLE INFO

Article history:
Received 9 March 2014
Received in revised form
17 June 2014
Accepted 14 July 2014
Available online 22 July 2014

Keywords:
PEM fuel cells
Gas diffusion layers
Membrane
Catalyst layer
Through-plane thermal conductivity
Thermal contact resistance

ABSTRACT

The thermal conductivity of the components of the membrane electrode assembly (MEA) and GDL must be accurately estimated in order to better understand the heat transfer processes in the proton exchange membrane (PEM) fuel cells. In this study, an experimental investigation has been performed to measure the through-plane thermal conductivity and the contact resistance for a number of gas diffusion layer (GDL) materials. The sensitivity of these quantities to the temperature, PTFE content and micro porous layer (MPL) coating has been undertaken. In addition, the through-plane thermal conductivity of the membrane has been measured and reported as a function of temperature and water content. Further, the through-plane thermal conductivity of the catalyst layer has been determined as a function of temperature and platinum loading. It has been found that the through-plane thermal conductivity of the components of the MEA decreases when the temperature increases, and the through-plane thermal conductivity of the GDL is significantly lower than its in-plane thermal conductivity.

© 2014 Elsevier B.V. All rights reserved.

1. Introduction

The thermal conductivity of the components of the membrane electrode assembly (MEA) and GDL must be accurately estimated in both directions, namely in-plane and through-plane directions, in order to better understand the heat transfer processes in proton exchange membrane (PEM) fuel cells [1–3]. Many researchers use a steady state method to measure the thermal conductivity of gas diffusion layers (GDLs) in the through-plane directions [4,5]. In particular, Vie et al. [6] were the first research group who attempted to measure the thermal conductivity of the fuel cell components. In their paper, many thermocouples have been inserted in the fuel cell and the temperature gradient is measured at different locations. The thermocouples were inserted between the gas diffusion layers, the catalyst layers and the membrane. The thermal conductivity of the E-Tek ELAT GDL and the catalyst layer was about $0.2 \pm 0.1\ W\ m^{-1}\ K^{-1}$. However, these measurements were not accurate due to the high uncertainty on the locations of the thermocouples and due to the fact that the thermocouples blocked some of the active area of the fuel cell. Khandelwal and Mench [7] measured the through-plane thermal conductivity of Toray and SIGRACET® carbon papers under 20 bar compression pressure. Ramousse et al. [8] estimated the thermal conductivity of a typical GDL to be lower than the thermal conductivity of pure carbon samples but they did not take into account the effect of the compaction pressure on the thickness of the sample. Nitta et al. [9] measured the thermal conductivity of SGL 10BA GDL and the thermal contact resistance between the GDL and the graphite rods. It was found that the values of the GDL thermal

* Corresponding author. Tel.: +44 113 343 5113; fax: +44 113 246 7310.
E-mail addresses: pm09neah@leeds.ac.uk, pm09neah@hotmail.com (N. Alhazmi).

http://dx.doi.org/10.1016/j.jpowsour.2014.07.082
0378-7753/© 2014 Elsevier B.V. All rights reserved.

conductivity obtained were almost 4 times larger than those found in the literature and it depends on the compression pressure on the sample. They reported the measured through-plane thermal conductivity of the GDL to be about 1.8 ± 0.11 W m^{-1} K^{-1}. Karimi et al. [10] determined the through-plane thermal conductivity of SpectraCarb GDL experimentally. The contact resistance between the GDL and the aluminium apparatus surface was studied as a function of compression and PTFE content. The results showed that as the compression load increases, the thermal conductivity of the GDL increases. The obtained through-plane thermal conductivity of the GDL was 0.36 and 0.7 W m^{-1} K^{-1}under a compression load 0.7 and 13.8 bar, respectively. Burheim et al. [11] reported that the through-plane thermal conductivity of dry GDLs and GDLs that contain water. The liquid water was sucked for about 30 s and the volume fraction of the water was calculated by comparing the weight of the dry and wet GDLs. Their results showed that the through-plane thermal conductivity of the GDL increases with the presence of liquid water and it is 0.15 and 1.6 W m^{-1} K^{-1} for the dry and wet GDL, respectively.

In this paper, an experimental setup, based on the steady-state method, is developed to measure the through-plane thermal conductivity of the components in the membrane electrode assembly (MEA) and GDL at different operating temperatures. The thermal conductivities of the GDLs are investigated as a function of the PTFE loading, temperature and compression pressure. In addition, for the present study to be comprehensive, the through-plane thermal conductivities of Nafion® membranes and catalyst layers are measured and reported as a function of the temperature.

2. Materials and procedures

2.1. Test apparatus

An experimental apparatus has been developed to measure the thermal conductivity of the various components of the MEA and GDL under steady state conditions. Therefore, the formula employed to estimate the thermal conductivity is the Fourier law [12]:

$$q_s = k_s A_s \frac{\Delta T}{L_S} \quad (1)$$

where A_S is the cross-sectional area of the sample, L_s is the length of the sample, k_s is the thermal conductivity of the sample, and ΔT is the temperature drop across the sample.

The test apparatus is shown in Fig. 1. It consists of, from top to bottom, (i) a dial gauge indicator to measure the reduction in the thickness of the sample under compression, (ii) a load cell which records the compression pressure on the sample, (iii) the upper steel flux metre, which contains 3 thermocouples, (iv) the tested sample, and (v) the lower steel flux meter which also contains 3 thermocouples whose temperature gradient is maintained low and constant using a cooling system, see Section 2.3 for more details.

2.2. Materials

The through-plane thermal conductivity of the GDL is determined for five different SGL samples (10AA, 10BA, 10CA, 10DA, 10EA) whose PTFE loading are 0, 5, 10, 20 and 30%, respectively. In addition, the effect of the micro porous layer (MPL) coating on the through-plane thermal conductivity has been investigated for two different samples, namely 10BC and 10BE, and the thermal conductivity of them has been compared with that of their base substrate, namely 10BA. These GDL samples, which were provided by the SGL Technologies Gm bH, Germany, are listed in Table 1.

The through-plane thermal conductivity of a 115 Nafion® 115 membrane (Du Pont, USA), which is about 127 μm thick, is also measured and reported. Furthermore, the through-plane thermal conductivity of the catalyst is evaluated with three different platinum (Pt) loadings, namely 0.2, 0.4 and 0.6 mg cm^{-2} in order to investigate the effect of this loading on the through-plane thermal conductivity of the catalyst layer.

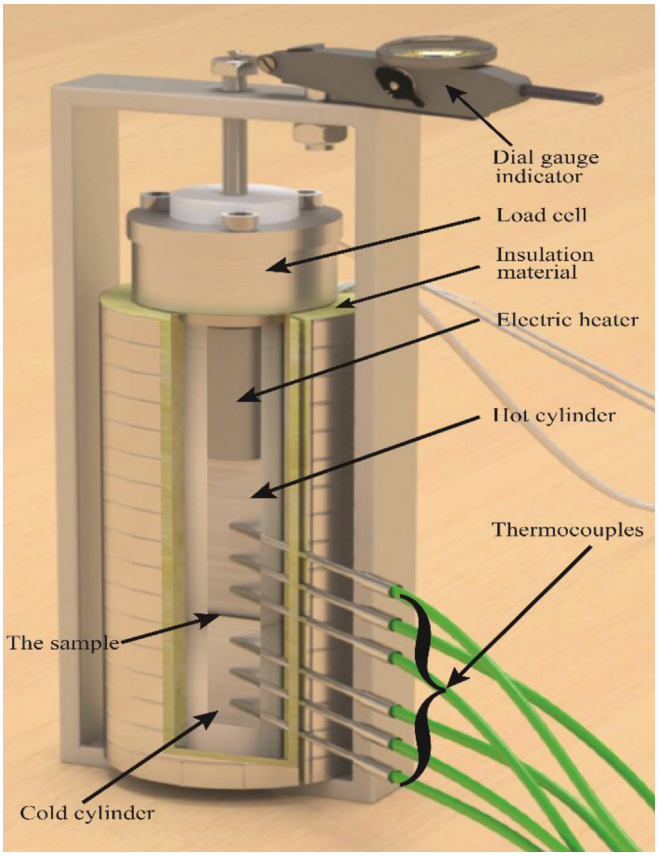

Fig. 1. Configuration of the experimental set-up to measure the through-plane thermal conductivity of the MEA components.

2.3. Experimental conditions

All measurements were performed under vacuum conditions in order to eliminate the heat transfer by convection. Moreover, the fixtures and the samples were well insulated by using Rockwool insulation to minimise the heat loss in the radial direction and mitigate heat transfer by radiation. The effect of the temperature on the through-plane thermal conductivity of all the components in the MEA and GDL was investigated in the temperature range 35–80 °C, which is the most likely operating temperature range of PEM fuel cells [13]. In addition, the effect of the compression pressure was investigated for the compression range 1–20 bar, in which the normally-used compressive pressure on PEM fuel cells

Table 1
Manufacturers' specifications for the tested GDLs.

GDL	Thickness (μm)	PTFE loading (wt. %)
10AA	390	0
10BA	400	5
10CA	400	10
10DA	400	20
10EA	374	30
10BC	415	23[a]
10BE	367	50[a]

[a] PTFE loading in the MPL (wt. %).

lies [14]. The lower steel cylinder was maintained cold by using EXT-440 Koolance's and CHC-122 cooling block through which the cooling fluid flows. All the thermocouple readings, the current, the voltage in the circuit and the pressure readings, were controlled and monitored by a LabVIEW application, see Fig. 2.

It is important to note that every measurement in this study was repeated at least twice in order to cheque for repeatability. If the results were not repeatable then further measurements were made until repeatable results were obtained.

2.4. Methodology

The axial heat flux through the tested samples was estimated by averaging the heat fluxes through upper and lower flux meters by using the following equations:

$$q_{\text{up}} = k_m \frac{T_1 - T_3}{L_1 - L_3} \tag{2}$$

$$q_{\text{low}} = k_m \frac{T_4 - T_6}{L_4 - L_6} \tag{3}$$

$$q_s = \frac{q_{\text{up}} + q_{\text{low}}}{2} \tag{4}$$

where q_s is the heat flux through the sample, q_{up} is the heat flux through the upper flux-metre, q_{low} is the heat flux through the lower flux-meter, k_m is the thermal conductivity of the standard material, and T_1, T_2, T_3, T_4, T_5, and T_6 are the temperatures measured by the first, second, third, fourth, fifth and the sixth thermocouples, respectively.

The temperature drop ΔT across the test sample is obtained by 'joining' the temperature gradients of the lower and upper fixtures, as shown in Fig. 3.

The total resistance, R_{Total}, to the heat flow, which is the sum of 'bulk' thermal resistance and the contact resistance [12], can be expressed using the Fourier equation as follows:

$$R_{\text{Total}} = \frac{\Delta T}{q_s} = 2R_{H-\text{sample}} + R_{\text{th}} \tag{5}$$

where R_{th} is the sample thermal resistance, $R_{\text{H-sample}}$ is the contact resistance between the sample and the holder, ΔT is the temperature drop across the sample, and q_s is the heat transferred through the sample which is given by Eq. (4). The thermal contact resistance is calculated from the total resistance for a single GDL as follows:

$$R_{\text{total}} = R_{\text{sample}} + 2R_{H-\text{sample}} \tag{6}$$

Since it is not feasible to estimate the contact resistance between the sample and the holder using a single sample with a given thickness, we need either to change the thickness of the sample used or use a stack of samples. However, it is significantly difficult to vary the thickness of the sample as typically the GDL is not available in different thicknesses. Alternatively, the thickness is varied by making stacks of different numbers of individual GDL samples and assuming that the contact resistance between the samples are the same [11]. However, this introduces a new variable, which is the contact resistance between individual samples. So, the total contact resistance for a stack of GDL samples is calculates as follows:

$$R_{\text{total},n} = nR_{\text{sample}} + (n-1)R_{\text{sample-sample}} + 2R_{H-\text{sample}} \tag{7}$$

In the current study, a stack of five GDL samples is used to vary the thickness of the tested specimens. This means that there will be five equations with three unknowns in order to ensure that the

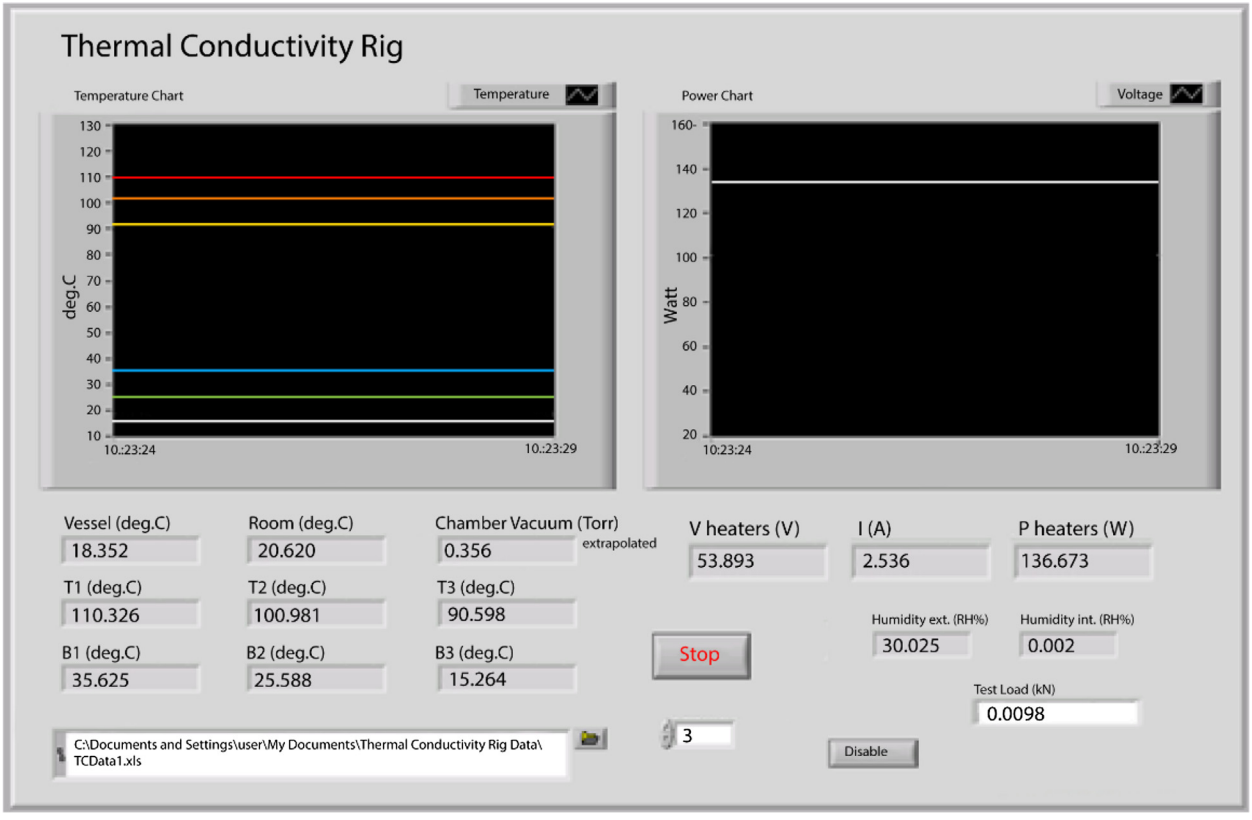

Fig. 2. The LabVIEW programme interface.

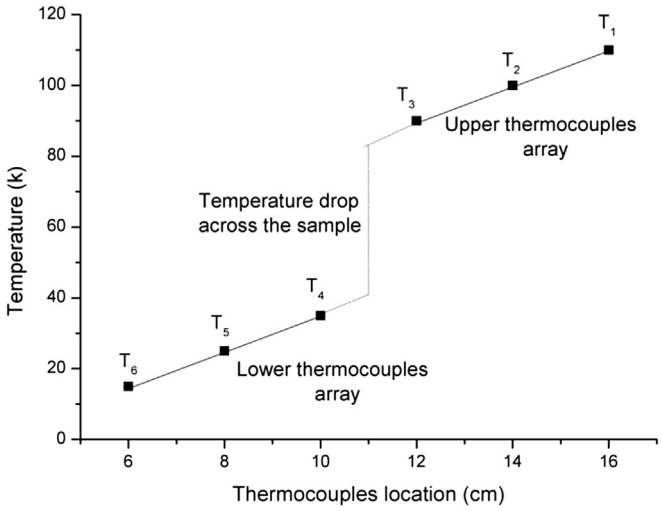

Fig. 3. A typical steady state temperature profile through the fixture.

assumption that the contact resistance between the samples are the same.

The thermal resistance offered by the sample is given by:

$$R_{\text{total},1} = R_{\text{sample}} + 2R_{H-\text{sample}} \tag{8}$$

The thermal resistance offered by the sample is given by:

$$R_{\text{th}} = \frac{L_s}{k_s A_s} \tag{9}$$

where L_s is the length of the sample, k_s is the thermal conductivity, and A_s is the heat transfer area [12]. For a given compression, the contact resistance between the GDL sample and the holder surface is assumed to be insensitive to the number of the samples involved in the stack. Then, the thermal conductivity of the sample k_s is calculated from the slope of the curve of the total thermal resistance as a function of GDL thickness:

$$k_s = \frac{1}{\text{slope}} \times \frac{1}{A_s} \tag{10}$$

2.5. Validation of the measurement technique

The experimental technique was validated by using a standard thin film material. The thermal conductivity of a stack of 27 ± 2.5 μm aluminium foils was measured to be about 236.3 ± 4.2 W m^{-1} K^{-1}, which was found to be in good agreement with the reported value for the thermal conductivity of aluminum foils, which is about 235 W m^{-1} K^{-1} at room temperature [15].

2.6. Uncertainty analysis

The uncertainty in the thermal conductivity values can be estimated based on the combined uncertainties in the dimensions of the sample, and the temperature drop across the sample [16] as follows:

$$\frac{\delta k}{k} = \sqrt{\left(\frac{\delta T_c}{T_c}\right)^2 + \left(\frac{\delta T_h}{T_h}\right)^2 + \left(\frac{\delta L}{L}\right)^2 + \left(\frac{\delta A}{A}\right)^2} \tag{11}$$

where T_c and T_h are the temperature of the cold and hot plates, respectively. L is the length of the sample and A is the sample cross sectional area.

The uncertainty in the through-plane thermal conductivity value is calculated and reported for all the measurements and it was not more than 8% in this study.

3. Results and discussions

3.1. Effect of the temperature on the through-plane thermal conductivity of the membrane

As seen in Fig. 4a, the through-plane thermal conductivity of the membrane is in good agreement with the in-plane thermal conductivity of the membrane, which has been previously measured by using the parallel thermal conductance technique which is based on the thermal resistance measurements from the parallel resistance circuit depends on the output power and the temperature drop through the sample [17]. The maximum through-plane thermal conductivity of the membrane was 0.193 ± 0.02 W m^1 K^{-1} when the temperature was 35 °C, and as the temperature increases then the thermal conductivity of the membrane decreases. For example, the minimum through-plane thermal conductivity of the membrane was 0.132 ± 0.02 W m^1 K^{-1} when the temperature was 80 °C.

This decrease in the thermal conductivity of the membrane is due to the increase in the thermal resistance of the membrane with temperature, as shown in Fig. 4b. Basically, the thermal

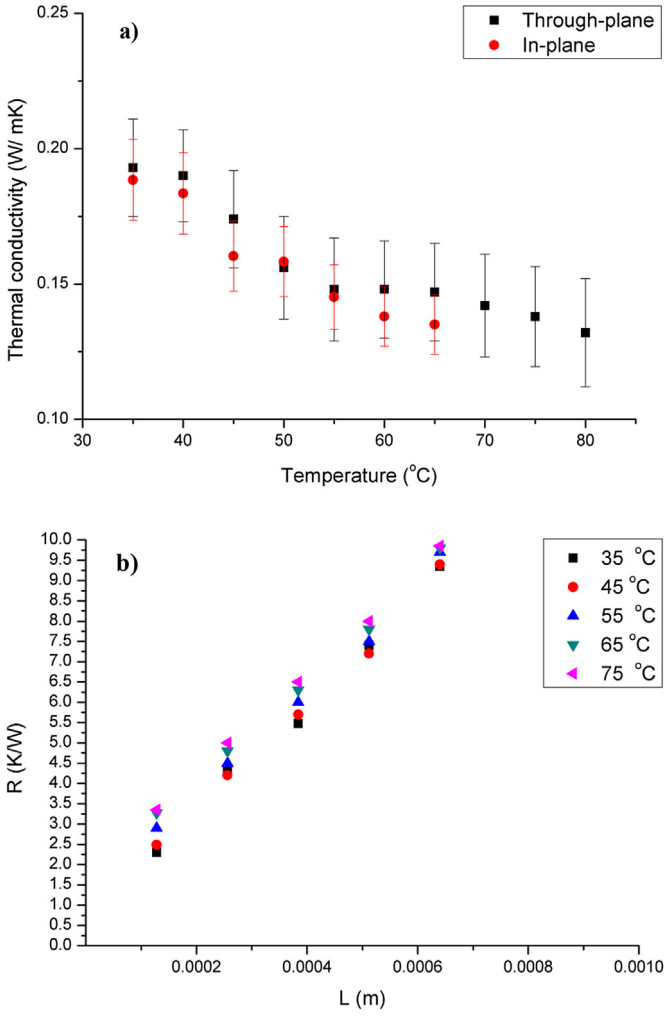

Fig. 4. Measured thermal conductivity and thermal resistance of the membrane as a function of the temperature along with the experimental error bars.

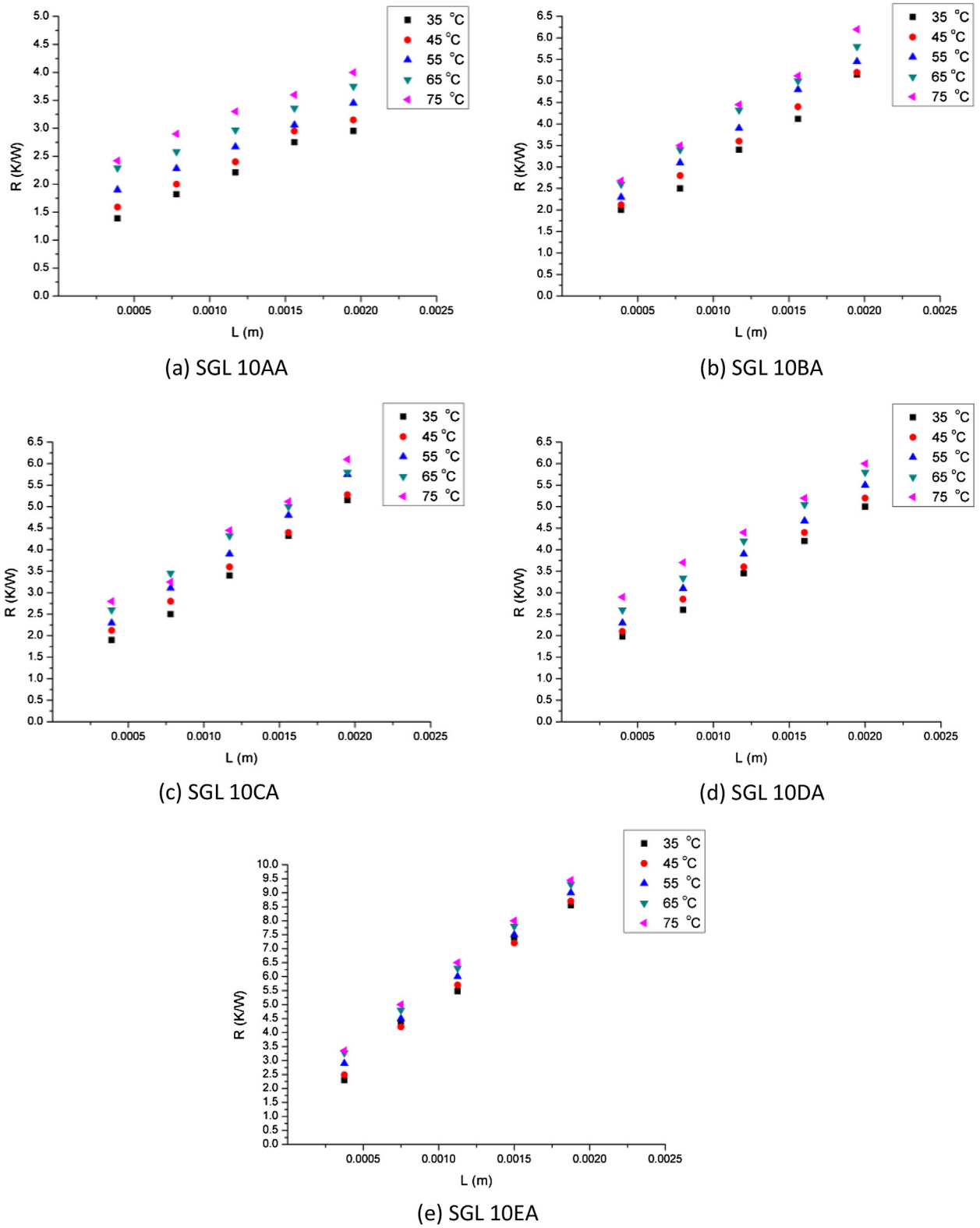

Fig. 5. Measured thermal resistances of the GDLs as a function of the temperature for (a) SGL 10AA, (b) SGL 10BA, (c) SGL 10CA, (d) SGL 10DA, and (e) SGL 10EA.

conductivity of the membrane decreases with increasing temperature due to the decrease in the phonon mean free path as a result of increasing the number of phonon at the high temperature for the polymers as Nafion material [18].

This relation is explained by using this equation [19]:

$$k_{\mathrm{mem}} = \frac{1}{3} c_{\mathrm{ph}} \nu_{\mathrm{ph}} l_{\mathrm{ph}} \tag{12}$$

where k_{mem} is the thermal conductivity of the membrane, l_{ph} is the phonon mean free path, c_{ph} is the phonon heat capacity and ν_{ph} the

phonon velocity. In the high temperature c_{ph} and v_{ph} are almost constants, while is l_{ph} decreases and consequently the thermal conductivity of the membrane decreases [20,21], which is considered as an insulating material.

3.2. Effect of the temperature on the through-plane thermal conductivity of the GDL

Due to the presence of the PTFE binder and the polymeric resin, whose thermal conductivities decrease with increasing temperature, the total thermal resistance of the GDL was found to increase with increasing temperature and subsequently the thermal conductivity decreases as the temperature increases [22]. This effect is clearly shown in Fig. 5.

3.3. Effect of the PTFE loading on the through-plane thermal conductivity of the GDLs

The through-plane thermal conductivity of GDL is significantly lower than its in-plane thermal conductivity [17]. For example, at 35 °C, the in-plane thermal conductivity of 10AA was found to be about 12.5 W m^{-1} K^{-1} [17] whereas the through-plane thermal conductivity of the same material at the same temperature was measured as 0.55 W m^{-1} K^{-1} at 2 bar. It should be noted that the compression has a positive effect on the thermal conduction, see Section 3.4.

Since the heat transfer is from fibre to fibre in the through-plane direction, the addition of PTFE decreases the through-plane thermal conductivity of the gas diffusion layer because of the low thermal conductivity of the PTFE, which is about 0.25 W m^1 K^{-1} [23–25].

As illustrated in Fig. 6, overall, the thermal conductivity of the GDL significantly decreases after PTFE-treatment. The GDL, without PTFE, has the highest through-plane thermal conductivity and its thermal conductivity is about 50% higher than that of the PTFE-treated GDLs. However, the real relation between adding PTFE and the through-plane thermal conductivity of the GDL is not clear as there was no significant difference in the through-plane thermal conductivity of the GDL after adding 5, 10, 20, and 30% PTFE to the GDL. This point certainly requires further investigation.

3.4. Effect of compression pressure on the through-plane thermal conductivity of the GDL

In PEM fuel cells, the GDL is deforming under the ribs and the thickness of the GDL under the ribs is less than its thickness under the channel. The GDL thickness is greatly affected by the external compression, which affects the transport properties, the contact resistance and the thermal and electrical conductivities of the GDL and these subsequently affect the temperature and the water management in PEM fuel cells [23]. Therefore, the effect of the compression on the thermal conductivity of the GDL is needed to be taken into account. The effect of compression pressure on the reduction in the thickness of the GDL is shown in Fig. 7.

The reduction in the thickness is initially very high when applying the compression pressure. Then, the variation in thickness is almost negligible after increasing the pressure which indicates that the deformation of the GDL has 'saturated'. Note that there is a hysteresis effect in the compression curves which signals that there has been a permanent deformation in the compressed GDL sample [26]. In Fig. 8a, the effect of the applied load on the thermal resistance has been investigated. It is clear that the thermal resistance values of the treated GDLs are higher than that of the untreated GDL. This is due to the increase in the contact resistance between the fibres of the GDL after adding the PTFE [27].

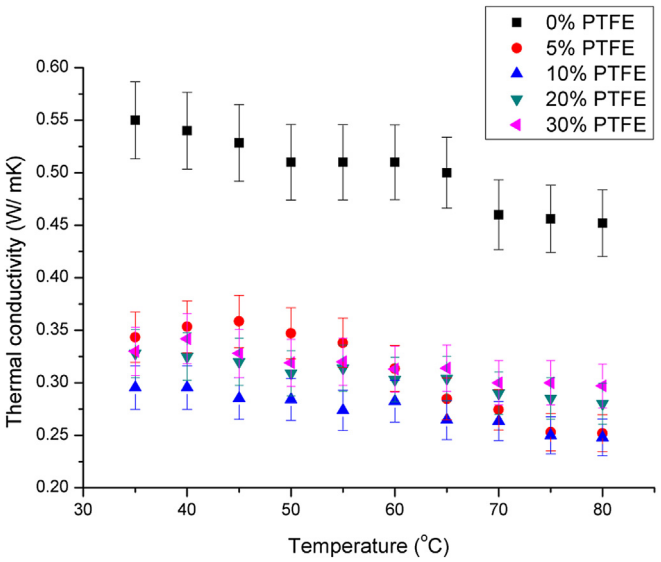

Fig. 6. Measured thermal conductivity of the GDLs as a function of the temperature and PTFE loading along with the experimental error bars.

The through-plane thermal conductivity of the GDL increases when the compression pressure increases, as shown in Fig. 8b. This is as a result of the larger contact area and consequently this provides more heat paths and thus the higher thermal conductivity [28]. It should be noted that these results are those of increasing compressive pressure.

3.5. Effect of the MPL coating on the through-plane thermal conductivity of the GDL

In order to enhance the water and thermal management in the PEM fuel cells, a micro porous layer (MPL) is added to the gas diffusion layer. This layer consists of a carbon black powder and hydrophobic agent [8].

The thermal contact resistance of the GDL samples decreases when the MPL is added to the GDL. This is not surprising as one of the main aims of adding MPL to the GDL in the fuel cell is to improve the contact between the GDL and the catalyst layer.

Furthermore, it is clear from Fig. 9 that the untreated 10BA has a lower thermal conductivity than that of 10BC and 10BE, which are MPL coated GDLs. The main reason for this is that the MPL is rich in carbon powder which is considered as a high thermal conductivity material compared to the thermal conductivity of the untreated GDL.

3.6. Effect of the temperature on the through-plane thermal conductivity of the catalyst layer

The through-plane thermal conductivity of the catalyst layer was investigated by manually spraying the Pt ink onto some 10BA GDL samples and then measure the through-plane thermal conductivity of the samples before and after adding the catalyst layer. Since the layers are lumped in series, the series model [29,30] illustrated in Fig. 10 was used to calculate the thermal conductivity of the catalyst, as follows:

$$k_{total} = \frac{1}{\frac{\nu_{cl}}{k_{cl}} + \frac{\nu_{GDL}}{k_{GDL}}} \tag{13}$$

where k_{total} is the thermal conductivity of the catalysed GDL. k_{GDL} and k_{cl} are the thermal conductivities of the GDL and catalyst layer,

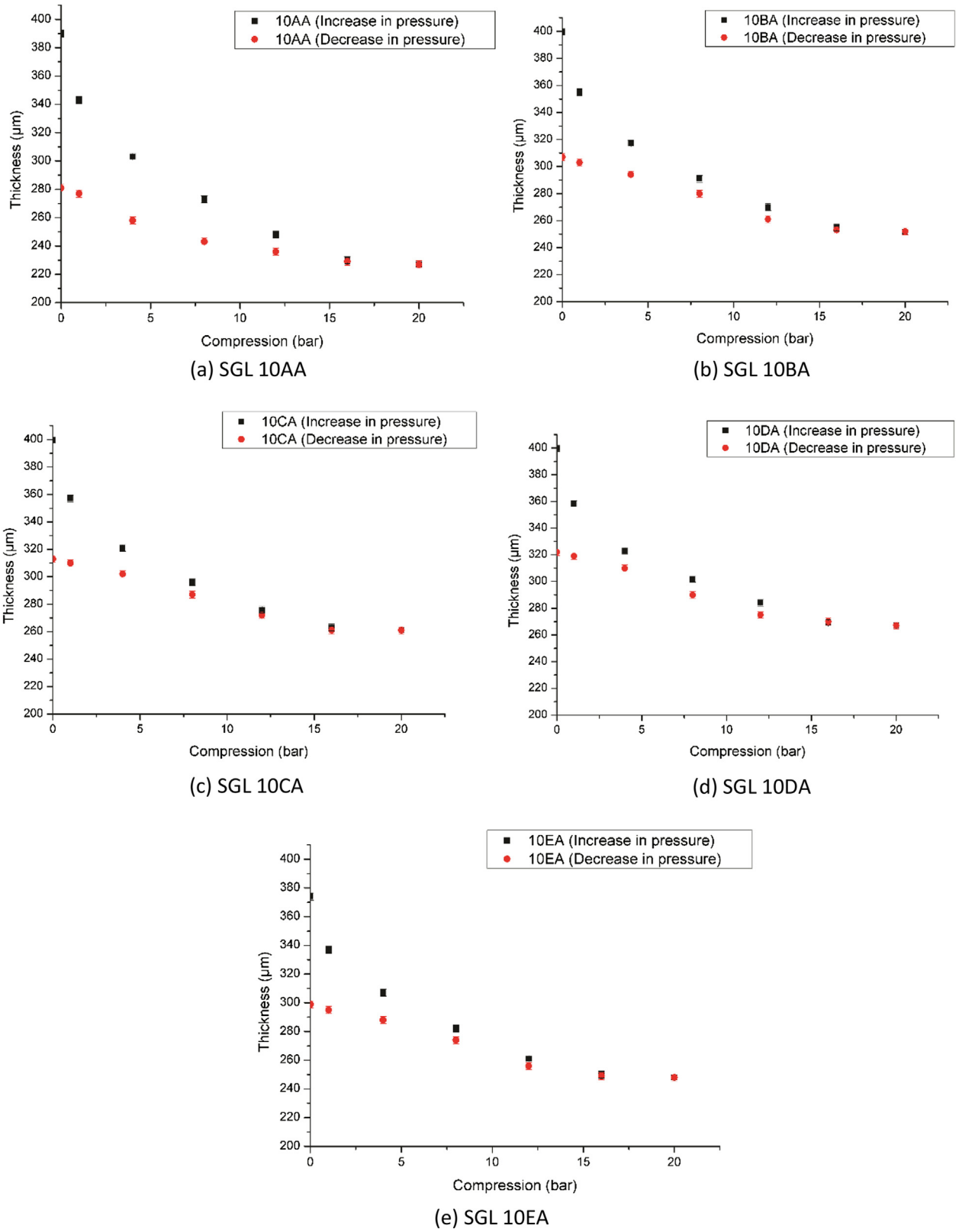

Fig. 7. Hysteresis in the thickness of the GDL under the external compression for (a) SGL 10AA, (b) SGL 10BA, (c) SGL 10CA, (d) SGL 10DA, and (e) SGL 10EA.

respectively. ν_{GDL} and ν_{cl} are the volume fractions of the GDL and catalyst layer, respectively.

As shown in Fig. 11, the through-plane thermal conductivity of the catalyst layer, with 0.4 mg cm^{-2} platinum loading, was found to be comparable with the in-plane thermal conductivity of the catalyst layer which has been previously measured and reported in Ref. [17]. This indicates that the catalyst layer is a homogenous material. Furthermore, the through-plane thermal conductivity of

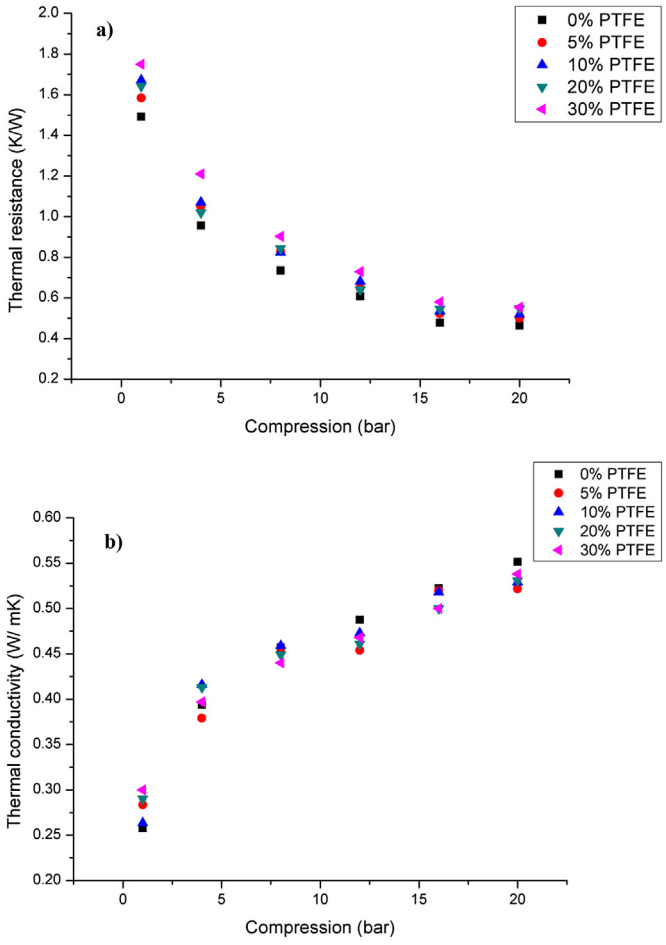

Fig. 8. Measured thermal conductivity and thermal resistance of the GDLs at different compression loads.

the catalyst layer was almost insensitive to the temperature. The maximum through-plane thermal conductivity of the catalyst layer is 0.345 ± 0.02 W m^{-1} K^{-1} when the temperature is 35 °C, and the minimum through-plane thermal conductivity of this catalyst layer is 0.334 ± 0.02 W m^{-1} K^{-1} when the temperature is 80 °C.

In order to investigate the effects of the Pt loading on the through-plane thermal resistance of the catalyst layer, the catalyst

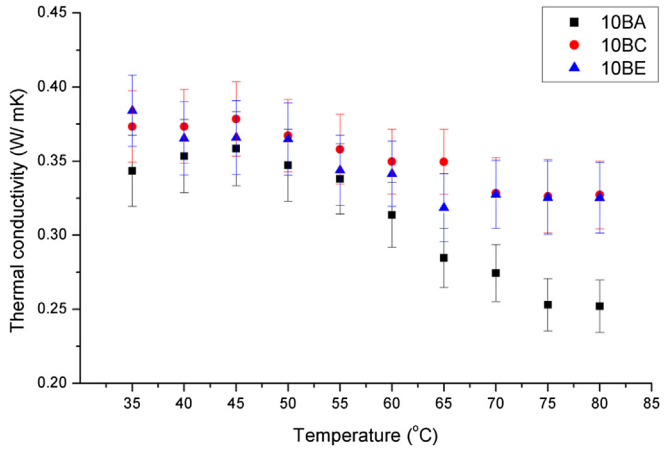

Fig. 9. Measured thermal conductivities for (a) SGL 10BA, (b) SGL 10BC, and (c) SGL 10BE along with the experimental error bars.

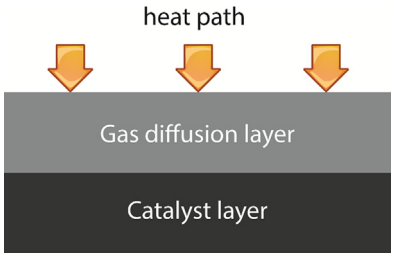

Fig. 10. Calculating the thermal conductivity of the catalyst using the series model.

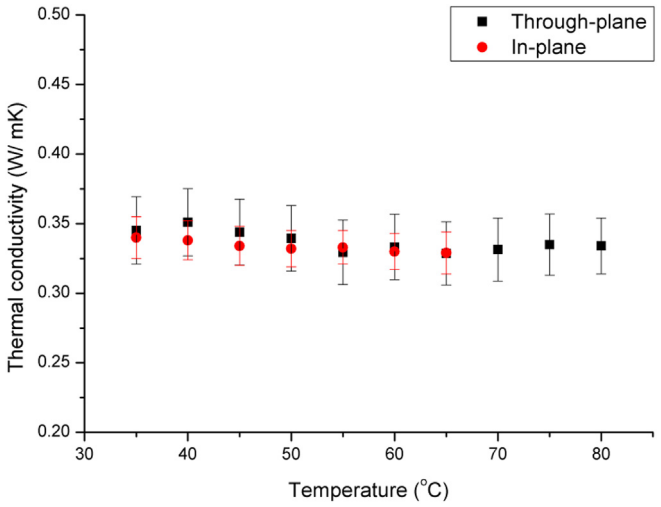

Fig. 11. Measured thermal conductivity of the catalyst layers as a function of the temperature along with the experimental error bars (the platinum loading for this case is 0.4 mg cm^{-2}).

layers with three different Pt loadings (0.2, 0.4, 0.6) mg cm^{-2} were prepared and the through-plane thermal resistance of them were compared, see Fig. 12.

The through-plane thermal resistance of the catalyst layer was found to decrease with Pt loading. This is mainly because of the thickness of the catalyst layer. As the platinum loading increases, the thickness of the catalyst layer increases. This leads to a better

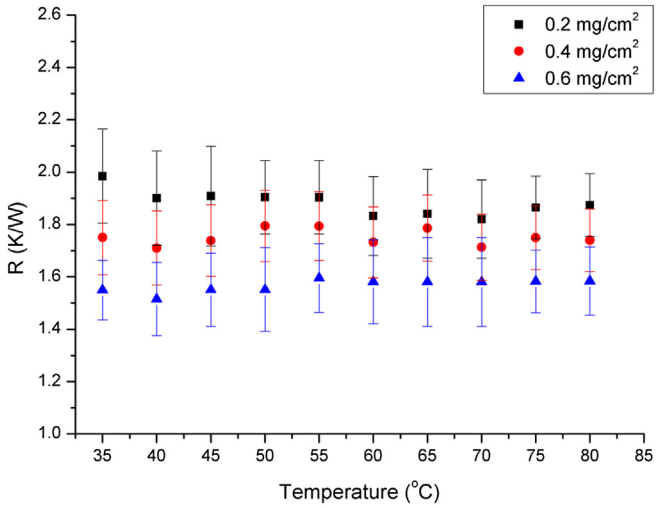

Fig. 12. Measured thermal resistances of the catalyst layers as a function of the Pt loading along with the experimental error bars.

contact between the catalyst layer and the holder of the sample. Therefore, the reduction in the total resistance as a result of increasing the platinum loading is more to do with the contact resistance and not with the thermal conductivity which must ideally remain constant.

4. Conclusions

In this study, an experimental technique has been developed to determine the through-plane thermal conductivity and the contact resistance of the components in the MEA and GDL. The main conclusions of these measurements are as follows:

- The through-plane thermal conductivity of the membrane was found to be comparable with the in-plane thermal conductivity and it decreases with increasing the temperature. The through-plane thermal conductivity of the membrane was found to be 0.193 ± 0.018 W m^{-1} K^{-1} and 0.132 ± 0.02 W m^{-1} K^{-1} when the temperature was 35 °C and 80 °C, respectively.
- The through-plane thermal conductivity of the GDL was found to be significantly lower than its in-plane thermal conductivity. The through-plane thermal conductivity of the GDL decreases with increasing the temperature and increases with increasing compression pressure.
- The through-plane thermal conductivity of the catalyst layer is comparable to its in-plane thermal conductivity and it was found to be almost insensitive to the temperature and the thermal resistance of the catalyst layer decreases slowly with Pt loading due to the increase in the thickness of the catalyst layer and the contact resistance. The through-plane thermal resistance of the catalyst layer, when the temperature was 35 °C, was found to be 1.985 ± 0.18 K W^{-1} and 1.553 ± 0.13 K W^{-1} when the Pt loading was 0.2 and 0.6 mg cm^{-2}, respectively.

The through-plane thermal conductivity of the GDL and the MEA components provides some of the necessary parameters which will enhance the predictions of the profiles of temperature and water saturation in PEM fuel cells. As a future work, it will be of great interest to measure the thermal conductivity of the components of the MEA beyond the temperature of 120 °C, which is normally the operating temperature for high-temperature PEM fuel cells.

Acknowledgement

The first author appreciates the financial support from the Ministry of Higher Education in Saudi Arabia and the technical assistance from Mr Paul Crosby and Mr Gurdev Bhogal in the Energy Technology Innovation Initiative at the University of Leeds.

Nomenclature

A	cross-sectional area of the sample (m^2)
c_{ph}	the phonon heat capacity (J g^{-1} K^{-1})
k_s	thermal conductivity of the sample (W m^{-1} K^{-1})
k_m	thermal conductivity of the standard material (W m^{-1} K^{-1})
k_{mem}	thermal conductivity of the membrane (W m^{-1} K^{-1})
k_{cl}	thermal conductivity of catalyst layer (W m^{-1} K^{-1})
k_{GDL}	thermal conductivity of GDL (W m^{-1} K^{-1})
l_{ph}	the phonon mean free path(m)
L_s	length of the sample (m)
q_{low}	heat transfer through the lower plate (W)
q_s	heat transfer through the sample (W)
q_{up}	heat transfer through the upper plate (W)
$R_{H\text{-}Sample}$	thermal contact resistance between two layers of the sample (m^2 KW^{-1})
$R_{Sample\text{-}Sample}$	thermal contact resistance between two layers of the sample (m^2 KW^{-1})
R_S	sample thermal resistance (K W^{-1})
R_{Total}	total thermal resistance (K W^{-1})
v_{ph}	the phonon velocity(m s^{-1})
T_1	temperatures measured by the first thermocouple (°C)
T_3	temperatures measured by the third thermocouple (°C)
T_4	temperatures measured by the fourth thermocouple (°C)
T_6	temperatures measured by the sixth thermocouple (°C)
T_C	cold plate temperature (°C)
T_h	hot plate temperature (°C)
ΔT	temperature drop (K)
ν_{cl}	volume fraction of catalyst
ν_{GDL}	volume fraction of GDL

Abbreviations

CL	catalyst layer
GDL	gas diffusion layer
MEA	membrane electrode assembly
MPL	micro porous layer
PEM	proton exchange membrane
PTFE	polytetrafluoroethylene

References

[1] G. Maggio, V. Recupero, C. Mantegazza, J. Power Sources 62 (1996) 167–174.
[2] T. Berning, D.M. Lu, N. Djilali, J. Power Sources 106 (2002) 284–294.
[3] M. Hamour, J.P. Garnier, J.C. Grandidier, A. Ouibrahim, S. Martermianov, Int. J. Thermophys. 32 (2011) 1025–1037.
[4] N. Zamel, X. Li, J. Shen, A. Wiegmann, J. Becker, Chem. Eng. Sci. 65 (2010) 3994–4006.
[5] S. Park, J.W. Lee, B.N. Popov, Int. J. Hydrogen Energy 37 (2012) 5850–5865.
[6] P.J.S. Vie, S. Kjelstrup, Electrochim. Acta 49 (2004) 1069–1077.
[7] M. Khandelwal, M. Mench, J. Power Sources 161 (2006) 1106–1115.
[8] J. Ramousse, O. Lottin, S. Didierjean, D. Maillet, Int. J. Therm. Sci. (2008) 1–6.
[9] I. Nitta, O. Himanen, M. Mikkola, J. Fuel Cell. Sci. 8 (2008) 111–119.
[10] G. Karimi, X. Li, P. Teertstra, Electrochim. Acta 55 (2010) 1619–1625.
[11] O. Burheim, P.J.S. Vie, J.G. Pharoah, S. Kjelstrup, J. Power Sources 195 (2010) 249–256.
[12] T.M. Tritt, Thermal Conductivity: Theory, Properties, and Applications, Kluwer Academic/Plenum Publishers, 2004.
[13] S. Karvonen, T. Hottinen, J. Ihonen, H. Uusalo, J. Fuel Cell. Sci. Tech. 5 (2008) 0410091–0410099.
[14] O.S. Burheim, J.G. Pharoah, H. Lampert, P.J.S. Vie, S. Kjelstrup, J. Fuel Cell. Sci. Tech. 8 (2010) 21013.
[15] J.E. Hatch, Aluminium: Properties and Physical Metallurgy, fifth ed., American Society for Metals. Metals Park, 1984.
[16] R.J. Moffat, Exp. Therm. Fluid Sci. 1 (1988) 3–17.
[17] N. Alhazmi, D. B Ingham, M.S. Ismail, K.J. Hughes, L. Ma, M. Pourkashanian, J. Power Sources 241 (2013) 136–145.
[18] C.L. Choy, Y.W. Wong, G.W. Yang, T. Kanamoto, J. Polym. Sci. Part B: Polym. Phys. 37 (1999) 3359–3367.
[19] L. Song, Y. Chen, J.W. Evans, J. Electrochem. Soc. 144 (1997) 3797–3800.
[20] K.A. Mauritz, R.B. Moore, Chem. Rev. 104 (2004) 4535–4585.
[21] Nafion Product Sheet, Dupont, USA, 2008.
[22] D.M. Price, M. Jarratt, Thermochim. Acta 392 (2002) 231–236.
[23] S. Escribano, J. Blachot, J. Ethve, A. Morin, R. Mosdale, J. Power Sources 156 (2006) 8–13.
[24] N. Zamel, E. Litovsky, S. Shakhshir, X. Li, J. Kleiman, Int. J. Hydrogen Energy 36 (2011) 12618–12625.
[25] J. Blumm, M. Meyer, C. Strasser, Int. J. Thermophys. 31 (2010) 1919–1927.
[26] E. Sadeghi, N. Djilali, M. Bahrami, J. Power Sources 195 (2010) 8104–8109.
[27] I. Nitta, O. Himanen, M. Mikkola, Electrochem. Commun. 10 (2008) 47–51.
[28] E. Sadeghi, N. Djilali, M. Bahrami, J. Power Sources 196 (2011) 246–254.
[29] M. Sahimi, Flow and Transport in Porous Media and Fractured Rock, Wiley, 2012.
[30] G. Dagan, Flow and Transport in Porous Formations, Springer, 1989.